Chemical Engineering Journal 390 (2020) 124627

Contents lists available at ScienceDirect

Chemical Engineering Journal

journal homepage: www.elsevier.com/locate/cej

Long-term validation of polyhydroxyalkanoates production potential from the sidestream of municipal wastewater treatment plant at pilot scale

Vincenzo Conca[a], Cinzia da Ros[a], Francesco Valentino[b], Anna Laura Eusebi[c], Nicola Frison[a,*], Francesco Fatone[c]

[a] Department of Biotechnology, University of Verona, Strada Le Grazie, 15-37134, Verona, Italy
[b] Department of Chemistry, "La Sapienza" University of Rome, P.le Aldo Moro 5, Rome 00185, Italy
[c] Department of Science and Engineering of Materials, Environment and City Planning, Polytechnic University of Marche, Ancona 60131, Italy

HIGHLIGHTS

- Sidestream PHA production was integrated with the treatment of anaerobic reject water.
- PHA represents up to 17.5% of the total COD recovered.
- Potential sidestream PHA production from municipal wastewater was 1.2 kgPHA/PE year.
- The integrated PHA production in WWTPs allows a potential revenue of 2.2–5.9 €/PE year.

GRAPHICAL ABSTRACT

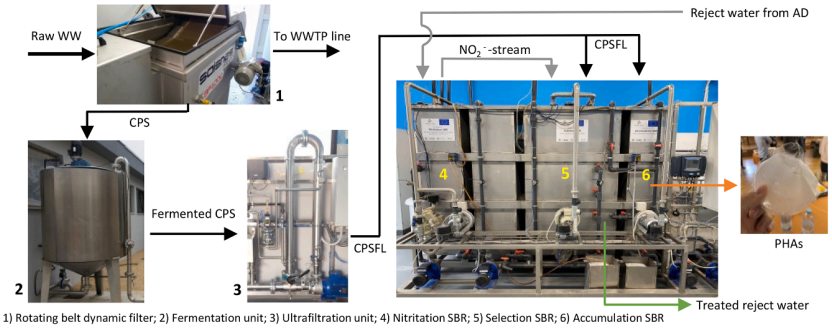

1) Rotating belt dynamic filter; 2) Fermentation unit; 3) Ultrafiltration unit; 4) Nitritation SBR; 5) Selection SBR; 6) Accumulation SBR

ARTICLE INFO

Keywords:
Anaerobic digestion
Volatile fatty acids
Water resource recovery facilities
Nitrogen removal
Bioplastics

ABSTRACT

In this study, polyhydroxyalkanoates (PHAs) production integrated with the via-nitrite nitrogen removal from anaerobic reject water was investigated at pilot scale under long-term period. The pilot plant was located in Carbonera wastewater treatment plant (WWTP) (Treviso, Italy) and comprised the following units: i) rotating belt dynamic filter (RBDF) for the recovery of cellulosic primary sludge (CPS); ii) fermentation unit for the production of volatile fatty acids (VFAs); iii) ultrafiltration unit (UF) for solid/liquid separation of the fermented sludge; iv) nitritation sequencing batch reactor (N-SBR) for the oxidation of ammonia to nitrite; v) selection SBR (S-SBR) where aerobic-feast and anoxic-famine conditions were established to select PHA-accumulating biomass and vi) an accumulation SBR (A-SBR) were intracellular PHA content was maximized through the feed-on-demand strategy. Results showed that around 80% of the influent ammonia was efficiently removed by the

Abbreviations: AD, anaerobic digestion; AOB, ammonium oxidizing bacteria; A-SBR, accumulation SBR; AUR, ammonium utilization rate; CH_4, methane; COD, chemical oxygen demand; COD_{SOL}, soluble COD; CPS, cellulosic primary sludge; CPSFL, cellulosic primary sludge fermentation liquid; DO, dissolved oxygen; FA, free ammonia; HRT, hydraulic retention time; MLVSS, mixed liquor volatile suspended solids; MMCs, mixed microbial cultures; NAR, nitrite accumulation rate; NH_4-N, nitrogen as ammonia; NO_2-N, nitrogen as nitrite; NOB, nitrite oxidizing bacteria; NO_x-N, nitrogen as nitrite and nitrate; N-SBR, nitritation SBR; OM, organic matter; ORP, oxydation reduction potential; PE, population equivalent; PHA, polyhydroxyalkanoates; PO_4-P, phosphorus as phosphate; RBDF, rotating belt dynamic filter; S/L, solid/liquid separation; SBFR, sequencing batch fermentation reactor; SBR, sequencing batch reactor; SRT, solid retention time; S-SBR, selection SBR; TKN, total kjieldahl nitrogen; TP, total phosphorus; TSS, total suspended solids; TVS, total volatile solids; UF, ultrafiltration; VFAs, volatile fatty acids; vNLR, volumetric nitrogen loading rate; vOLR, volumetric organic loading rate; VSS, volatile suspended solids; WAS, waste activated sludge; WRRF, water resource recovery facility; WW, wastewater; WWTP, wastewater treatment plant; Xa, active biomass

* Corresponding author.
E-mail address: nicola.frison@univr.it (N. Frison).

https://doi.org/10.1016/j.cej.2020.124627
Received 17 December 2019; Received in revised form 28 February 2020; Accepted 29 February 2020
Available online 02 March 2020
1385-8947/

system when both N-SBR and S-SBR operated with volumetric nitrogen loading rate (vNLR) of 1.64–1.72 kgN/m^3 d and 0.60–0.63 kgN/m^3 d, respectively. Accumulation tests showed PHA yields ranging between 0.58 and 0.61 g COD_{PHA}/g $COD_{VFA,}$ indicating an effective selection strategy. The overall mass balance assessment demonstrated that around 0.32 g of COD per gram of COD treated can be recovered as bio-based products. The integration of nitrogen removal and PHA production in the sidestream resulted in a methane recovery up to 4.0 m^3CH_4/PE y and a maximal PHA production of 1.2 kgPHA/PE y with a potential revenue for the WWTP up to 6.5 €/PE y.

1. Introduction

Over the last decades, a lot of efforts have been directed to change the paradigm of WWTPs from an end-of-pipe infrastructure to WRRFs. In this new paradigm, wastewater (WW) is considered as a renewable resource from which water, energy and materials can be recovered [1]. Biogas production has been widely adopted to partially offset the energy consumption for wastewater treatment [2]. However, the low value and energy content of the CH_4 has led to the development of new technologies aiming at the upgrade of the OM to a higher value bioproducts [3]. In recent years, great interest has been given to PHAs production due to their wide application as environmental-friendly bioplastics [4]. These biopolymers are completely biodegradable and produced by over 300 bacterial species as carbon and energy reserve [5]. Their biosynthesis is usually stimulated by the presence of excess carbon in concomitance with the absence of macronutrients (i.e. nitrogen or phosphorus) or transient excess of soluble carbon without any nutrient limitation (i.e. feast/famine environment [6]). Commercial PHAs production currently uses expensive sources of OM and pure bacterial consortium, increasing the production costs from around two to five times in comparison with fossil-fuel based plastics [7]. In 2014, the PHA market price varied between 4 and 5 €/kg from the high-value medical product to low-value consumables for agricultural purpose [8]. A recent forecast of the European Bioplastics Association [9] showed an increase of the PHA production capacity up to 6 times more by 2024. To fill this gap, the use of open mixed- instead of pure-cultures and low-cost carbon sources could be considered a valid alternative due to the large interest gained over the last years. The typical process for MMCs PHAs production usually comprises three different steps: i) acidogenic fermentation for VFAs production, ii) selection of biomass with significant PHA production capability and iii) accumulation to maximize the intracellular PHA content. Nevertheless, although fundamentals and methods for PHA production from MMCs have been largely published in literature, the technology readiness level (TRL) still remains low (i.e. < 5 [3]). Moreover, a suitable PHA extraction and purification process has not been identified yet, although several techniques were investigated in literature [7,10]. In any case, the type of recovery technique has to be selected according to the desired properties and purity which will also affect the selling price in the market.

To date, few studies on MMC-PHAs production at pilot scale from different feedstocks have been reported in literature. Anterrieu et al. [11] investigated the integration of PHAs production with wastewater treatment in a Dutch sugar factory, while Valentino et al. [12] described a biorefinery for the conversion of the organic fraction of municipal solid waste (OFMSW) and WAS into PHAs. In another work, Bengtsson et al. [13] studied the feasibility of PHAs production from municipal wastewater treatment with biological carbon and nitrogen removal. In that study, the carbon source for PHAs production was obtained from the acidogenic fermentation of an agro-industrial residual feedstock coming from local green-house tomato production. However, in all of these works, industrial and/or non-municipal organic contributions were evaluated, hindering the assessment of the actual PHA production potential from sole municipal wastewater. On the other hand, Morgan-Sagastume et al. [14] investigated the integrated municipal wastewater and sludge treatment with PHA production. The authors applied a feast/famine process in a pilot-scale SBR where the carbon source for the selection of PHA-accumulating biomass consisted of readily biodegradable soluble carbon present in raw WW. In the same study seasonal variability of WW characteristics were found, which implies a possible disadvantageous process instability from an industrial perspective. Based on previous pilot-scale results, Morgan-Sagastume et al. [15] reported the first techno-environmental assessment for the integration of PHA production with municipal WW treatment. The authors considered four different WWTP scenarios for carbon source production and biological nutrients removal. The results showed that the overall organic carbon conversion in WWTPs (0.26 gCOD/gCOD treated) was the same when AD was applied by itself or in combination with PHAs production. However, parameters for process design and estimation of potential PHA production from municipal wastewater itself have not been reported yet.

To boost the driver for conversion of WWTPs into WRRFs, an integrated PHA recovery via-nitrite from the sidestream treatment in WWTPs has been proposed by Frison et al. [16]. Coupling PHAs production within the treatment of more concentrate streams could represents a suitable option, since it decreases: i) volumes that needs to be managed; ii) costs for nutrients removal in the main line and iii) it ensures higher process stability due to the more stationary characteristics of these sidestream flows. The importance of optimizing the fermentation yields for VFAs production is crucial to increase the sustainability of the process. Lee et al. [17] reported yields between 85 and 300 $mgCOD_{VFA}$/gVSS when sole primary sludge was fermented. Crutchik et al. [18] investigated the use of CPS to maximize carbon diversion and its further valorization through VFAs production. Highest VFAs yield of 340$mgCOD_{VFA}$/$gTVS_{fed}$ has been found, underlining the potential of this substrate for on-site carbon source production. More recently, the use of CPS for several purposes, including VFAs production, has been investigated at pilot scale by da Ros et al. [19]. Fermentation yields up to 322$mgCOD_{VFA}$/$gTVS_{fed}$ in a sequencing batch fermentation reactor were reported, and different scenarios for CPS valorization were considered. The authors found that upgrading VFAs derived from CPS into high added value products such as PHAs would significantly increase the revenue of WWTPs, highlighting the importance of carbon diversion towards the development of WRRFs.

The present study is aimed to validate the long-term operation of an innovative pilot-scale plant integrating the via-nitrite nitrogen removal with PHAs production from the sidestream of Carbonera WWTP (Treviso, Italy). A novel substrate derived from fermentation of CPS was used as carbon source to evaluate the impacts on PHAs production. Each process unit was investigated to assess the long-term stability of the process and to define the parameters required for the full-scale implementation. Moreover, the overall mass balance was accomplished to answer to the following question: what is the actual PHAs production potential from sole municipal wastewater in the sidestream of WWTPs?

2. Materials and methods

2.1. Carbonera WWTP

The pilot plant was located inside of the Carbonera WWTP (Treviso, northern Italy). The full-scale plant had a treatment capacity of 40,000 PE and treated around 15,000 m^3/day of municipal wastewater without any industrial contribution. The water line was composed by

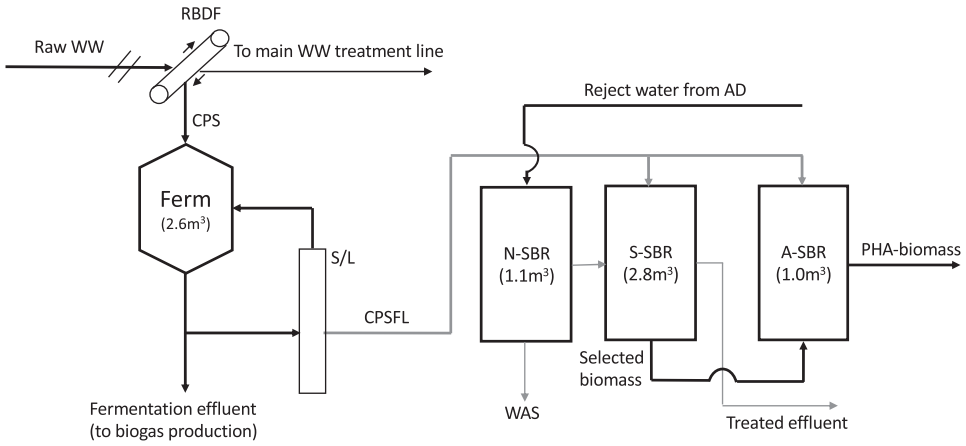

Fig. 1. Schematic representation of the pilot plant.

preliminary treatments, primary sedimentation, biological reactor (Schreiber process), secondary sedimentation, disinfection and final filtration. The sludge line was composed by a static pre-thickener followed by dynamic thickening (installed during the experimental period) of mixed primary and secondary sludge, equalization tank for thickened sludge, anaerobic digester and the Short-Cut Enhanced Nutrients Abatement (S.C.E.N.A.) system for the treatment of sludge reject water [20].

2.2. Process units and flowchart

The pilot plant treated around 10% (1.5–3.0 m^3/day) of the daily produced anaerobic reject water, while the system comprised of six different units, as reported below:

1) RBDF for the recovery of CPS; 2) SBFR for the production of VFAs by acidogenic fermentation;3) UF unit for S/L; 4) N-SBR; 5) S-SBR; 6) Fed-batch accumulation reactor (A-SBR).

The flowchart of the process is reported in Fig. 1.

The scheme reported above was adapted from a previous study [16], in which the carbon source (VFAs) were produced by the acidogenic fermentation of mixed primary and secondary sludge instead of CPS from wastewater sieving as in this work.

2.3. Characteristics of the anaerobic reject water

The whole experiment lasted more than 600 days and three different experimental periods were identified on the basis of both the characteristics of the anaerobic reject water and the operating conditions of the system. Period 1 was between days 1–84, period 2 between days 170–319 while period 3 between days 370–613. On the other hand, the characteristics of the anaerobic reject water has been mainly affected in period 2 and 3 by the implementation of the dynamic thickening of sewage sludge. The latter increased the suspended solids concentration from 2.5% up to 5.0% on dry matter. The complete characteristics of the anaerobic reject water were reported in the Table 1.

2.4. SBFR for VFAs production from CPS

The SBFR (TA, Italy) was composed by a stainless-steel tank (AISI 304) with a total volume of 3.0 m^3. The working volume was kept at 2.6 m^3 and the temperature was maintained at 37 °C by an electrical heating system with an installed power of 1.5 kW. CPS was recovered through a RBDF (SF1000, Salsnes Filter, Norway) which operated with a mesh size of 350 μm in both period 1 and 2, while in period 3 a mesh size of 210 μm was installed. The operating mechanism of the RBDF is described in da Ros et al. [19]. The HRT of the fermenter varied between 4 and 6 days, the pH was not controlled, while the mixed liquor was kept under continuous agitation by a mixer (Motovario TH80B4, Italy) at 20 rpm. Before entering the UF unit, the fermented sludge was screened by a basket filter (SATI filter, Cesena, Italy) with a porosity of 3 mm and a volume of 5 L. The fermented cellulosic primary sludge was filtered by the S/L unit which was constituted by seven ceramic membranes, each one with 8 tubular channels with a porosity of 0.2 μm and a specific surface area of 0.2 m^2 (Sepra, Cesano Maderno, Italy). The membranes operated with an internal recycle flowrate of 30–35 m^3/h and the working pressure ranged from 3.5 to 4 bar and 1.5–2 bar in the inlet and effluent part of the membrane, respectively, resulting in flux of around 100 L/m^2 h of permeate that was then stored in a tank with a volume of 1 m^3. The characteristics of CPSFL are reported below (Table 2).

2.5. Nitritation SBR

The N-SBR consisted in a stainless-steel SBR with a working volume of 1.1 m^3. The operating cycle was composed by the following phases:

Table 1
Characteristics of the reject water during the different periods.

Parameter	Unit	Period 1 (days 1–84) Average ± st.dev	Period 2 (days 170–319) Average ± st.dev	Period 3 (days 379–613) Average ± st.dev
Dynamic thickening of sewage sludge	–	NO	YES	YES
COD	mgCOD/L	284 ± 104	1855 ± 713	1116 ± 303
COD_{SOL}	mgCOD/L	56 ± 11	1613 ± 620	970 ± 224
VFAs	mgCOD/L	ND	547 ± 149	64 ± 14
TKN	mgN/L	449 ± 34	1300 ± 168	1187 ± 119
NH_4-N	mgN/L	401 ± 31	1161 ± 150	1060 ± 106
TP	mgP/L	24.9 ± 3.8	25.2 ± 4.0	27.8 ± 8.3
PO_4-P	mgP/L	23.0 ± 3.1	23.3 ± 3.7	25.7 ± 7.7

Table 2
Characteristics of the CPSFL during the experimental periods.

Parameter	Unit	Period 1 and 2 Average ± st.dev	Period 3 Average ± st.dev
pH	–	4.8 ± 0.1	4.9 ± 0.2
COD_{SOL}	mgCOD/L	8786 ± 1568	12830 ± 1529
VFAs	mgCOD/L	8347 ± 1754	9975 ± 1984
Acetic Acid	mgCOD/L	2086 ± 317	2892 ± 301
Propionic Acid	mgCOD/L	4424 ± 356	5087 ± 428
Butyric Acid	mgCOD/L	1042 ± 237	1273 ± 185
Valeric Acid	mgCOD/L	795 ± 55	723 ± 89
COD_{VFA}/COD_{SOL}	%	86 ± 3	77 ± 6
$C_3/(C_2 + C_3)$*	mol/mol	0.52 ± 0.06	0.49 ± 0.08
NH_4-N	mgN/L	326 ± 23	290 ± 19
PO_4-P	mgN/L	70 ± 12	72 ± 15

* C2: VFAs species with even number of carbons; C3: VFAs species with odd number of carbons

idle, feeding, aerobic, settling and discharge. The SBR was inoculated by taking the sludge from the biological reactor of the main wastewater treatment line and the adopted strategy for AOB enrichment was to maintain a level of FA always higher than 1.5 mg NH_3/L to foster the nitrite oxidizing bacteria (NOB) washout [21]. The anaerobic reject water was pumped from an equalization tank (90 m^3) through a volumetric pump (Sydex, Lonigo, Italy) with a flowrate of 3.6 m^3/h, while the effluent was withdrawn through a centrifuge pump (Lowara, Milan, Italy) with a flowrate of 6 m^3/h in an equalization tank with a volume of 1.4 m^3. The reactor was equipped with probes (Hach-Lange, Germany) for the monitoring of the process, in particular conductivity, pH and dissolved oxygen (DO). Four ultra-fine bubble diffusers (INVENT, USA) were placed at the bottom of the reactor and oxygen was provided through a centrifuge blower (Mapro, Vincenza, Italy) with a flowrate of 17–20 m^3/h and controlled at 1.5 ± 0.5 mg O_2/L through a manual valve installed on the pipe for air supply. The pH was controlled at 7.5–8.0 by automatic addition of 30% NaOH (w/v) through a peristaltic pump. Temperature was not controlled during the first part of the experimental period, while a heating system was installed after period 1. Steady state conditions were considered when the NAR (Eq. (1)) was > 95% for approximatively 3x solids retention time (SRT).

$$NAR(\%) = \frac{NO_2^-}{NO_2^- + NO_3^-} \text{ x } 100 \quad (1)$$

In Table 3 the operating conditions of N-SBR among the different periods under steady-state conditions are reported.

2.6. Selection SBR

The S-SBR consisted in a stainless-steel SBR with a total volume of 2.8 m^3 and operated under (aerobic)-feast and (anoxic)-famine conditions. The operating cycle was composed by four different phases that occurred as follow: idle, feast, famine, settling and discharge. The selection strategy for the start-up was to apply a feast/famine ratio lower than 0.2 min/min, since this had been reported as a limit value to sustain a microbial consortium that will accomplish excess PHAs storage over growth [22,23]. The seed sludge was the same as for the N-SBR. Oxygen was provided during feast conditions by a centrifuge blower (Mapro, Vicenza, Italy) and ten ultrafine bubbles diffusers (INVENT, USA) placed in the bottom of the tank. Two probes (Hach-Lange, Germany) were installed within the reactor for the monitoring of ORP and DO. The blower was controlled by a variable frequency drive (VFD) to maintain a DO concentration of 2 ± 0.2 mgO_2/L, resulting in a flowrate between 25–60 m^3/h. The bulk liquid was mixed under anoxic conditions through a mixer (Motovario TH80B4, Modena, Italy) with a speed of 100 rpm. At the beginning of the cycle (feast phase), the carbon source was fed through a centrifuge pump (Lowara, Milan, Italy) with a flowrate of 6 m^3/h, while the effluent from N-SBR was pumped from the equalization tank to the S-SBR through a centrifuge pump (Lowara, Milan, Italy) with a flowrate of 6 m^3/h as soon as the famine phase started. In this way, nitrite was used as electron acceptor for biomass growth [16] during the denitrification. The treated effluent from S-SBR was finally discharged at the end of the cycle by a pneumatic valve. Steady state conditions were considered when the length of the feast phase remained constant for at least for 3x SRT. The operating conditions of the S-SBR during the different periods are reported in Table 4.

2.7. PHA accumulation tests

The maximum accumulation potential of the biomass was evaluated by several accumulation batches fed according with a multiple pulse-feeding strategy [12]. The accumulation reactor (A-SBR) consisted in a stainless-steel tank with a volume of 1 m^3 which operated as a fed-batch reactor. The reactor was equipped with a DO probe (Hach-Lange, Germany) and three ultra-fine bubble diffusers (INVENT, USA) placed at the bottom of the tank which provided oxygen through a centrifuge blower (Mapro, Vicenza, Italy) with a flowrate of 17 m^3/h. The excess sludge from the S-SBR was transferred to the A-SBR at the end of the cycle. The accumulation trials lasted between 6 and 7 h and the carbon source was added based on feed-on-demand strategy using DO as control parameter [24], according to an initial COD concentration of around 0.7–1.2 g COD_{VFA}/L to prevent any substrate inhibition as reported by Valentino et al. [12].

2.8. Analytical methods and online measurements

All the signals from the different units were continuously recorded through a Programmable Logic Controller (PLC, S7-1200, Siemens, USA) which also controlled the whole operation of the system.

Analytical samples were taken daily from both the N-SBR and S-SBR and, only during the accumulation tests, in the A-SBR. TSS and VSS, COD, COD_{SOL}, TKN and TP were determined according to Standard Methods [25,26]. Nitrites, nitrates and phosphates were determined by high performance ion chromatography (Dionex ICS-900 with AG14 column and AMMS 300 suppressor) on filtered samples (0.2 μm, Whatman syringe filters). VFAs were determined through an Agilent 6890 N gas chromatograph (GC) equipped with a flame ionization detector (FID) with a temperature of 230 °C and an Agilent J&W DB-FFAP

Table 3
Operating conditions of the N-SBR.

Parameter	Unit	Period 1* Average ± st.dev	Period 2 Average ± st.dev	Period 3 Average ± st.dev
Heated	–	NO	YES	YES
Temperature	°C	18.9 ± 2.1	26.6 ± 1.4	25.5 ± 1.7
SRT	day	13–15	22–25	22–25
HRT	day	0.99 ± 0.2	0.82 ± 0.16	0.73 ± 0.13
vNLR	kgN/m^3 day	0.64 ± 0.35	1.60 ± 0.26	1.62 ± 0.25
vOLR	kgCOD/m^3 day	0.06 ± 0.01	1.78 ± 0.11	0.68 ± 0.05
Cycles	n°/day	5.0 ± 1.2	4.5 ± 0.2	4.8 ± 0.2

* Only pseudo steady-state conditions were achieved (days 10–47)

Table 4
Operating conditions of the S-SBR.

Parameter	Unit	Period 1* Average ± st.dev	Period 2 Average ± st.dev	Period 3 Average ± st.dev
Heated	–	NO	YES	YES
Temperature	°C	18.8 ± 2.1	25.4 ± 1.4	26.8 ± 1.7
SRT	day	6–7	6–7	6–7
HRT	day	2.3 ± 0.6	2.0 ± 0.2	1.7 ± 0.2
tot vNLR	kgN/ m^3 d	0.18 ± 0.05	0.60 ± 0.14	0.63 ± 0.12
vNO_2-NLR	kgN/m^3 d	0.05 ± 0.03	0.47 ± 0.12	0.49 ± 0.11
vNO_x-NLR	kgN/m^3 d	0.14 ± 0.01	0.48 ± 0.12	0.50 ± 0.11
vOLR	kgCOD/m^3 d	0.89 ± 0.11	1.31 ± 0.07	1.58 ± 0.10
$vOLR_{VFA}$	$kgCOD_{VFA}/m^3$ d	0.77 ± 0.12	1.15 ± 0.07	1.22 ± 0.11
COD_{SOL}/NO_x-N	kgCOD/kgN	6.36 ± 2.4	2.73 ± 0.21	3.17 ± 0.24
COD_{VFA}/NO_x-N	kgCOD/kgN	5.51 ± 2.3	2.41 ± 0.18	2.49 ± 0.22
Cycles	n°/d	2.1 ± 0.6	2.5 ± 0.6	2.7 ± 0.3

* Only pseudo steady-state conditions were achieved

fused silica capillary column (15 m × 0.53 mm × 0.5 mm) using hydrogen as gas carrier. The instrument operated with a ramp temperature from 80 to 200 °C using 2-ethylbutyric acid as internal standard. Samples were prepared before GC analysis through filtration (0.2 μm, Whatman syringe filters) and acidification at pH 2 with orthophosphoric acid. The quantification of each carboxylic acid was carried using a calibration curve built using the analytical standard Volatile free Acid Mix (Merck KGaA, Germany).

For PHA quantification, each sludge sample (5.0 mL) was pretreated with a sodium hypochlorite solution (1.0 mL; 5% active chlorine) and placed in a freezer at −20 °C. The PHA quantification was carried out by using a gas chromatographic method, based on the acid methanolysis with acidified methanol (3% v/v H_2SO_4). The acidic hydrolysis of PHA followed by the methyl derivatization reaction generated volatile monomers, the methyl esters of 3-hydroxybutyric (3HB) and 3-hydroxyvaleric (3HV) acids.

The sample preparation procedure involved a thawing, centrifugation (8.500 rpm, 20 min) removal of the supernatant and quantitative transfer of the solid residue into pyrex glass tubes with 2.0 mL of the acidified methanol solution containing benzoic acid (0.05 g/L) as an internal standard. Then, 1.0 mL of $CHCl_3$ was added and the whole was digested for 4 h at 100 °C. After cooling, the addition of 1.0 mL of distilled water and the mixing generated two separate aqueous and organic phases. For the analysis, 1.0 μL of organic phase was injected into the gas chromatograph based on the method illustrated in [27].

The abundance of 3HB-3HV monomers were quantified using P (3HB-co-3HV) Sigma-Aldrich standard polymer at 5 wt% HV content.

2.9. Calculations

Nitrogen mass balances were calculated according to Battistoni et al. [28], while FA at different temperatures was calculated according to Anthonisen et al. [21]. For the calculation of Ammonia Utilization Rate (AUR, mg N/L h), ammonia profile was plotted over time using a linear regression analysis. The specific AUR (mg N/g VSS h) was calculated by normalizing the AUR for the Xa concentration (VSS in the case of N-SBR). In this study, VFAs were expressed as mg COD/L and were considered as the sum of the different species as reported by Frison et al [16]. The feast/famine ratio was calculated as the ratio between the length of the feast phase and the length of the famine phase, according to the following equation (Eq. (2)):

$$\text{Feast/Famine (min/min)} = \frac{\text{T feast}}{\text{T famine}} \quad (2)$$

where T famine is considered the period (aerobic and/or anoxic conditions) of the cycle between the complete depletion of the VFAs and the end of the anoxic phase. The PHA concentration was converted into COD according to the following oxidation stoichiometry: 1.67 g COD/g HB and 1.92 g COD/g HV. The total concentration was calculated as the sum of PHB and PHV (eq.3):

$$\text{PHA (mgCOD/L)} = \sum (\text{PHB+PHV}) \quad (3)$$

The PHA content within the biomass was expressed considering the equation:

$$\text{PHA (\%)} = \frac{\text{gPHA}}{\text{gVSS}} \text{ x } 100 \quad (4)$$

The concentration of Xa in both S-SBR and A-SBR was calculated by subtracting the concentration of PHA (g/L) from the concentration of VSS (g/L). Xa was then converted into COD by the stoichiometric value of 1.42 g COD/g Xa as reported by Tchobanoglous et al. [29].

The VFAs utilization rate (-qVFA, mg COD/g Xa h), was calculated by dividing the concentration of VFAs consumed with the duration of the feast phase. PHA storage yield ($Y_{PHA/VFA}$, g COD_{PHA}/g COD_{VFA}) and growth yield ($Y_{X/VFA}$, g Xa/g COD_{VFA}) were determined according to the following equations (eq.5 and eq.6):

$$Y_{PHA/VFA} = \frac{gCOD_{PHA} \text{ produced}}{gCOD_{VFA} \text{ consumed}} \quad (5)$$

$$Y_{X/VFA} = \frac{\text{VSS-PHA (g/L)}}{COD_{VFA} \text{ consumed (g/L)}} \quad (6)$$

3. Results and discussion

3.1. Performances of the nitritation SBR

The reactor was operated for more than 600 days globally. In order to accomplish a proper selection of the PHA-accumulating biomass, an adequate amount of electron acceptor (nitrite in this work) should be fed in the S-SBR. In the specific case, the design parameters of the N-SBR considered a daily production in the range of 1.2–1.5 kg NO_x-N/d with a nitrification efficiency of about 85% and a NAR higher than 95%, resulting in a vNO_2-NLR in the selection stage of 0.4–0.6 kg NO_2-N/m^3 d and residual ammonia to favor the growth of the PHA-accumulating biomass. The nitrite load in the S-SBR derived from a previous study conducted by Frison et al. [16], in which a similar nitrite loading rate in a lab-scale reactor with a comparable configuration to the present work was applied. The table below resumes nitrogen mass balances and oxidation efficiencies of N-SBR.

As shown above, the amount of nitrite produced was different among the different periods. Indeed, after the start-up in period 1, the combination of shorter SRT and low temperature resulted in the production of only 0.16 kgNO_2-N/d, which was quite lower production compared to the demands of the S-SBR. In period 1, although the nitrification efficiency was about 81.6% (Table 5) the NAR was only 32.6%, indicating a not established a complete via-nitrite pathway. However, the daily amount of produced NO_x was about 0.49 kgNO_x-N/

Table 5
Nitrogen mass balances and oxidation efficiencies of the N-SBR.

Parameter	Unit	Period 1	Period 2	Period 3
		Average (Min-Max)	Average (Min-Max)	Average (Min-Max)
tot NLR in	kg N/d	0.69 (0.21–1.39)	1.80 (1.02–2.29)	1.89 (1.21–2.73)
NH_4-NLR in	kg N/d	0.63 (0.15–1.31)	1.64 (0.95–2.07)	1.72 (1.06–2.54)
NH_4-NLR out	kg N/d	0.12 (0.01–1.12)	0.18 (0.01–0.71)	0.30 (0.02–0.61)
NO_2-NLR out	kg N/d	0.16 (0.03–0.58)	1.31 (0.64–1.52)	1.35 (0.77–1.80)
NO_x-NLR out	kg N/d	0.49 (0.10–1.10)	1.33 (0.65–1.59)	1.36 (0.77–1.83)
X-NLR out	g N/d	9.8 (9.1–11.3)	16.7 (13.2–23.4)	10.4 (7.8–11.9)
Ammonia oxidation efficiency				
Nitrification Eff	%	81.6 (70.0–99.5)	88.9 (45.0–99.5)	82.5 (62.9–98.8)
NAR	%	32.6 (4.6–52.7)	98.5 (94.7–99.8)	99.2 (97.6–99.9)

d. The low NAR perhaps was due to the growth of NOB, probably fostered by the low concentration of FA inside the reactor due to the low operating temperature, which decreased at 14.9 °C after 38 days of operation. Under these conditions, the FA levels inside the reactor at the beginning of the cycle were found to be slightly lower than 2 mg NH_3/L, that could apparently be enough for NOB inhibition (0.1–1 mg NH_3/L [16]). However, Shao et al. [30], reported inhibition of NOB activity by *Nitrospira* only at FA levels between 1.83 and 9.61 mg NH_3-N/L. This indicated that since FA decreased throughout the cycle, the inhibiting conditions for NOB metabolism were no more present, justifying the observed nitrate accumulation. On the other hand, as reported by Salehizadeh and Van Loosdrecht [31], the rate of PHB degradation during the famine phase is independent from the type electron acceptor, meaning that either oxygen, nitrite or nitrate are suitable for the anabolic biomass metabolism under famine conditions. In any case, mass balances showed that the daily amount of produced NO_x-N would have not been enough for the S-SBR demand (1.2–1.5 $kgNO_x$-N/d). In addition, assuming that enough nitrates would have been produced, a higher amount of carbon source for complete PHA-driven denitrification in the selection stage would have been required. Indeed, the targeted COD/N for nitrite denitritation was set at 2.5 $gCOD_{VFA}/gNO_2$-N [16], but this value would have been 40% higher with nitrate as electron acceptor [29]. This would result in a reduction of substrate availability for PHAs production in the following accumulation step if no external carbon source addiction would be considered in real WWTPs. The best performances were observed in period 2 and 3 due to the higher amount of produced nitrite (1.31 and 1.35 kg NO_2-N/d as average value), according to a vNLR of 1.64–1.72 kgN/m^3 d and a NAR of 98.5 and 99.2% respectively. The higher nitrite productivity was attributed to the higher operational temperatures of the N-SBR and the increase of the SRT from 15 to 22–25 days. On one hand, this behavior seems to be in contrast with other literature studies, where the application of SRT lower than 5 days was shown to enhance AOB selection and NOB washout in synthetic municipal wastewater [32]. On the other hand, Jubany et al. [33] reported that complete via-nitrite pathway was achieved in a three aerobic reactors system connected in series treating extremely high strength (3000–4000 mg NH_4-N/L) synthetic wastewater operating with an SRT of 30 days. In this case, the key parameters for NOB washout was found to be a right combination of FA levels, low DO concentrations (1.2–1.9 mg O_2/L) and temperature (25 °C). Considering the very similar operating conditions of N-SBR, it was clear that a stable via-nitrite pathway was more suitable in period 2 and 3, respectively. The different operational conditions of the N-SBR reflected the effluent characteristics. Indeed, the nitrite concentration showed an average value of 111, 946 and 857 mg NO_2-N/L, while the nitrate concentration was 207, 13 and 7 mg NO_3-N/L for period 1, 2 and 3 respectively.

At the same time, different AUR value were observed due to the different operating conditions. As reported in Table 6, during the first period, the AUR showed an average value of 22.3 mg N/L h, with a specific AUR (at 20 °C) of 16.2 mg N/g VSS h. The latter was slightly higher than the one reported for period 2 (14.3 mg N/g VSS h), probably due to the lower presence of residual biodegradable COD in the anaerobic reject water (e.g. VFAs), which is a suitable well-known substrate for the growth of heterotrophic bacteria. However, it is important to underline that the observed AUR in period 2 was equal to 55.7 mg N/L h, almost three times higher compared to the previous period. Considering a similar daily aeration time for all the monitoring campaign (21.4 h/d on average), the more favorable operating conditions in period 2 (e.g. controlled temperature) resulted in a most consistent mass of ammonia effectively converted to nitrite every day. In the last period, the observed AUR was very similar compared to period 2, but the sAUR (at 20 °C) was 70% higher with an observed value of 22.5 mg N/g VSS h. This was due to the increase in the stability of the AD process with consequent decrease in soluble COD in the anaerobic supernatant, which resulted in a lower growth of heterotrophic biomass in period 3.

3.2. Performances of the S-SBR

The S-SBR was started up after the achievement of pseudo steady-state conditions in the N-SBR (day 17), to ensure an adequate amount of electron acceptor for a proper PHA-accumulating biomass selection. The feast/famine and aerobic/anoxic trends among the different experimental periods were reported in Fig. 2(a–c).

After the start-up in period 1, the feast to famine ratio decreased from about 0.15 min/min to around 0.09 min/min in 10 days. However, the $T_{feast}/T_{aerobic}$ ratio decreased from around 1 min/min to the minimum value of 0.11 min/min after 47 days. This was due to the extension of the aeration time, caused by the lack of electron acceptor provided by the N-SBR during the first experimental period. Indeed, the applied vNO_2-NLR was only 0.05 kg NO_2-N/m^3 d while the vNO_x-NLR was 0.14 kg NO_x-N/m^3 d. Considering the latter value, it is clear that it was quite lower compared with the potential capacity of the system,

Table 6
Kinetics of AUR in the different periods (average and standard deviation were calculated within days 10–47 for period 1, days 200–319 for period 2 and days 407–613 for period 3).

Parameter	Unit	Period 1 Average ± st.dev	Period 2 Average ± st.dev	Period 3 Average ± st.dev
AUR_{obs}	mgN/l h	21.6 ± 3.4	55.7 ± 6.2	56.4 ± 5.8
sAUR	mgN/gVSS h	15.9 ± 3.1	15.4 ± 4.2	25.6 ± 3.4
sAUR (20 °C)	mgN/gVSS h	15.7 ± 2.9	13.2 ± 4.1	22.5 ± 3.3

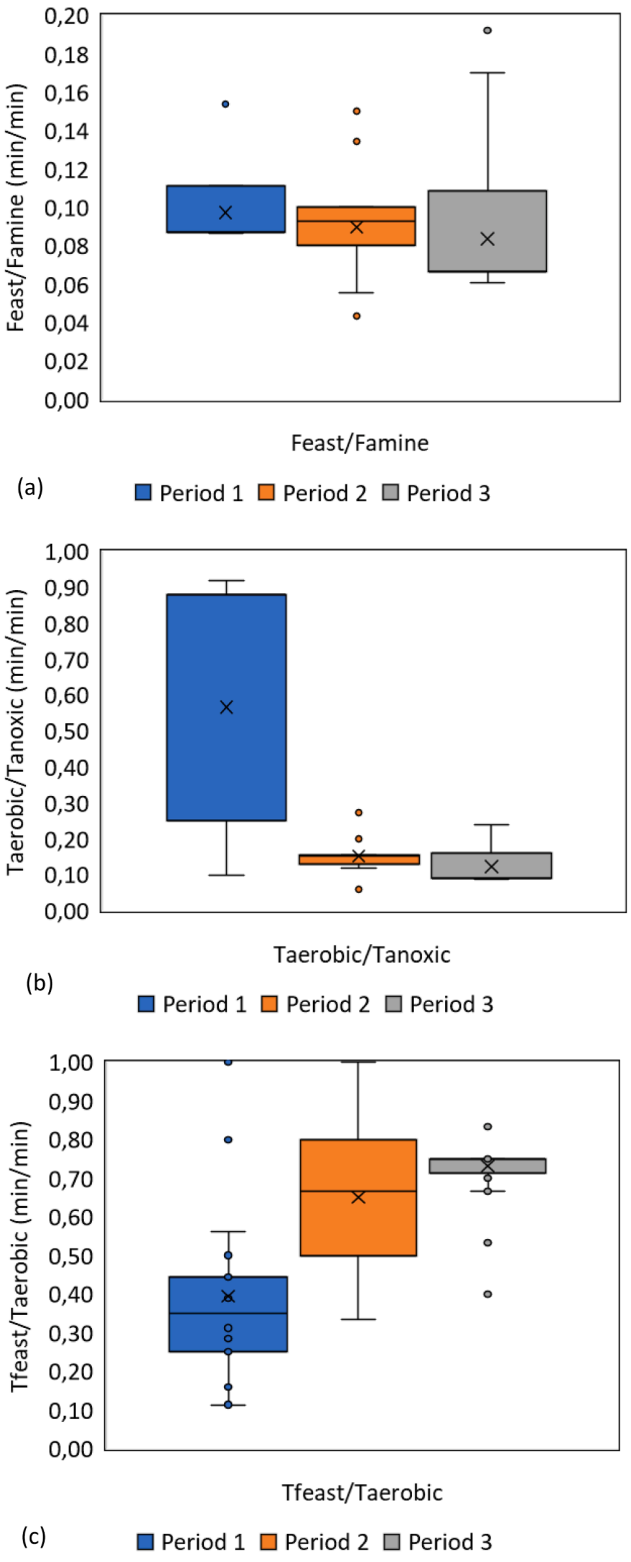

Fig. 2. a). Feast to famine ratio; b) Taerobic/Tanoxic ratio; c) TFeast/Taerobic ratio.

justifying the need of an aerobic phase duration extension. In this way, after the depletion of VFAs at the end of feast phase, aerobic famine conditions were established within the reactor for the remaining aeration time ($T_{aerobic}$-T_{feast}). This resulted in an increase of the $T_{aerobic}$/T_{anoxic} ratio up to 0.92 min/min (Fig. 2b), indicating that anoxic famine conditions accounted only for about 44% of the total cycle length.

In periods 2 and 3 instead, the feast/famine ratio showed a quite constant average value of 0.09 min/min after the start-up (Fig. 2a). The operating conditions of the S-SBR were similar in both periods and resulted in an average $T_{feast}/T_{aerobic}$ ratio of 0.65 and 0.73 min/min in period 2 and 3, respectively (Fig. 2c). Although these values could still appear low, it must be noticed that the length of the aerobic feast phase of the cycle was set according to the changes in the DO profiles, due to the decreased oxygen consumption rate during the famine phase as reported by Wang et al. [34]. Taking into account the variability of the carbon source characteristics, it was decided to extend the aerobic phase of 10–15 min after the increase of DO concentration, in order to avoid residual VFAs concentration at the beginning of the anoxic famine phase. However, in period 2 and 3, the $T_{aerobic}/T_{anoxic}$ ratio decreased to 0.15 and 0.13 min/min respectively, resulting in a famine phase effectively accomplished for more than 94% under anoxic conditions (Table 7). The vNO_x-NLR was efficiently increased up to 0.74 and 0.71 kg NO_x-N/m^3 d in period 2 and 3, however showing an average value of 0.47 and 0.49 kg NO_2-N/m^3 d, respectively.

The substrate uptake rate has been calculated during the whole monitoring period, since it was strictly connected with the feast to famine ratio. As shown in Fig. 3, the $-q_{VFA}$ increased from 60 to 100 mg COD/g Xa h up to 419, 477 and 485 mg COD/g Xa in period 1, 2 and 3, respectively. It is widely reported that PHA producers take advantage from their high velocity in substrate consumption over conventional heterotrophic growers [35]. Thus, it was clear that the selection strategy within the process was successful. In fact, the average $-q_{VFA}$ was quite similar all over the periods with a value of 301, 322 and 289 mg COD/g Xa h for period 1, 2 and 3, respectively. These results are higher with the one observed by Frison et al. [16] in a lab scale SBR, mainly due the higher SRT applied (12–15 day) which resulted in an average $-q_{VFA}$ of 239 mg COD/g Xa h operating under aerobic-feast and anoxic-famine conditions. However, after day 500 (period 3) a slight increase in the biomass concentration in concomitance with a simultaneous decrease in the substrate uptake rate was observed (Fig. 3). This behavior was attributed to the increase of the non-VFAs fraction and other biodegradable soluble COD in the carbon source, which is known to foster the growth of non PHA-accumulating biomass [12]. The average Xa concentration in the first period was equal to 1.4 g Xa/L, which decreased to 0.49 g Xa/L on day 82. This reduction was due to the lower biological activity consequently to the drop of the operating temperature up to 11 °C, resulting in both lower substrate uptake rate and growth of biomass. On the other hand, in period 2 and 3, the average biomass concentration was respectively recovered up to 2 g Xa/L and 2.5 g Xa/L, due to more suitable operating conditions. Indeed, the temperature increase in combination with the higher nitrite availability, favored the growth of PHA-accumulating biomass under strictly aerobic-feast and anoxic-famine conditions. The $Y_{PHA/VFA}$ under feast conditions was higher than 0.70 g COD_{PHA}/g COD_{VFA} in both period 1 and 2, while was lower in period 3, as shown in the table below (Table 8).

The lower $Y_{PHA/VFA}$ in period 3 was attributed to the growth of non PHA-accumulating biomass able to consume the biodegrable non-VFA fraction of COD in the carbon source. However, comparing the Y_{PHA}^{feast} with the studies of Valentino et al. [12,36], which operated a pilot-scale SBR for PHA production from fermented feedstock with comparable COD_{VFA}/COD_{SOL} ratio under aerobic dynamic feeding (ADF), it seemed that the accomplishment of aerobic-feast and anoxic-famine conditions translated into a higher selective pressure, increasing the PHA yields under feast conditions. On the other hand, this behavior could have been a consequence to the fact that the applied vOLR in this study (0.7–1.5 kg COD/m^3 d) could determine a “low-OLR enrichment strategy”, according to the conditions described by Albuquerque et al. [37]. Indeed, the same study reported a higher storage response over growth under vOLR lower than 2.5 kg COD/m^3 day in an SBR operating

Table 7
Summary of feast/famine ratio and distribution among the different periods.

Parameter	Unit	Period 1 Average. ± st.dev	Period 2 Average. ± st.dev	Period 3Average. ± st.dev
T_{feast}	min/cycle	55 ± 19	47 ± 14	44 ± 19
T_{famine}	min/cycle	527 ± 146	543 ± 142	484 ± 74
Feast/famine	min/min	0.10 ± 0.01	0.09 ± 0.02	0.09 ± 0.03
$T_{feast}/T_{aerobic}$	min/min	0.39 ± 0.24	0.65 ± 0.17	0.73 ± 0.07
$T_{aerobic}/T_{anoxic}$	min/min	0.52 ± 0.13	0.15 ± 0.04	0.13 ± 0.07
Aerobic famine/total famine	%	31.6 ± 9.7	5.3 ± 1.9	3.7 ± 1.4
Anoxic famine/total famine	%	68.4 ± 11.6	94.7 ± 1.8	96.3 ± 1.5

under ADF with fermented molasses as carbon source. In addition, Korkakaki et al. [38] reported PHA yields up to 0.84 g COD_{PHA}/g COD_{VFA} under feast conditions in an SBR enriched under carbon-limiting conditions (vOLR < 1.5 kg COD/m^3 day). These results can highlight the fundamental role that this parameter, in combination with the novel (aerobic)-feast/(anoxic)-famine, could have played in the PHA-accumulating biomass selection strategy of the present study.

As regard as the F/M, the S-SBR operated under similar value during both period 1 and 2, while decreased slightly in period 3 were an average value of 0.49 g COD_{VFA}/g Xa d was observed. On the other hand, the Y_{obs} of the PHA-accumulating biomass ranged from 0.29 to 0.31 g X_a/g COD_{VFA} (Table 8). Considering the SRT applied in the present study, these values were in agreement with the theoretical yields based on data reported in Henze et al. [39] of 0.31 g Xa/g COD_{VFA}. However, despite the similar Y_{obs} observed during the whole monitoring period, supposing a certain PHA content (e.g. 35–40% w/w), the lower amount of available biomass for the accumulation step in period 1, due to the lower applied vOLR, would have reduced the potential PHA productivity of the system, thus limiting the overall process performances.

3.3. Perfomances of the via-nitrite nitrogen removal

Taking into account the $Y_{PHA/VFA}$ under feast conditions and the NAR, the applied COD_{VFA}/NO_x-N ratio threshold was calculated to ensure an average denitritation efficiency of around 85%.

The low NO_x availability in the first period resulted in an average applied vOLR of 0.77 kg COD_{VFA}/m^3 d, corresponding to a COD_{VFA}/NO_x-N ratio of 5.51 g COD_{VFA}/g NO_x-N. In both period 2 and 3, instead, the average vOLR was increased at 1.15 and 1.22 kg COD_{VFA}/m^3 d and the COD_{VFA}/NO_x-N was 2.41 and 2.49 gCOD_{VFA}/g NO_x-N, respectively (Fig. 3). The higher COD_{VFA}/NO_x-N ratio in period 1 was consequence of the over extension of the aerobic phase, where some intracellular PHA was supposed to be consumed for biomass growth under aerobic conditions, instead of anoxic ones.

A satisfactory denitritation efficiency was not fully reached in period 1 (74.5%), while was successfully achieved in both periods 2 and 3 where an average efficiency of 87.7 and 86.0% was respectively observed (Fig. 4). Despite the similar efficiencies, the low NO_x-N loading rate of period 1 resulted in a low mass of removed nitrogen (~0.34 kg N/d), compared to period 2 and 3, where around 1.1–1.2 kg N/d were efficiently removed. However, if a higher denitritation efficiency should be required, it has been calculated that a COD_{VFA}/NO_x-N ratio of 2.8–2.9 should be applied to the system if the NAR in the N-SBR is higher than 95%. This value is only 20–25% higher than the amount of the carbon source required for conventional denitritation (2.2–2.3 g COD_{VFA}/gNO_2-N [40]), highlighting the technology potential for carbon valorization through integrated PHA production and nitrogen removal.

A slight decrease in the denitritation efficiency was observed in the middle of period 3 (from day 500). This behavior was found to be in concomitance with the decrease in the substrate uptake rate as well as a small reduction in the COD_{VFA}/NO_x-N ratio. These phenomena were probably connected, supporting the hypothesis that the presence of some non-VFA fraction in the carbon source favored the growth of non PHA-accumulating biomass, thus reducing the carbon availability for the denitritation driven by PHA. Specifically, although the COD_{VFA}/NOx-N ratio was almost similar in period 2 and 3, the COD_{sol}/NO_x-N ratio was 16% higher in period 3. The overall nitrogen removal efficiencies under steady-state conditions (periods 2 and 3) were 79.9 and 77.5%, respectively, when the applied nitrite loading rate was equal to 0.47 and 0.49 kg NO_2-N /m^3 d. These performances were slightly better compared to the work of Frison et al. [16] where a nitrogen removal efficiency of 79% was found using sludge fermentation liquid as carbon source, but with an applied total vNLR of 0.42 kg NO_2-N/m^3 d.

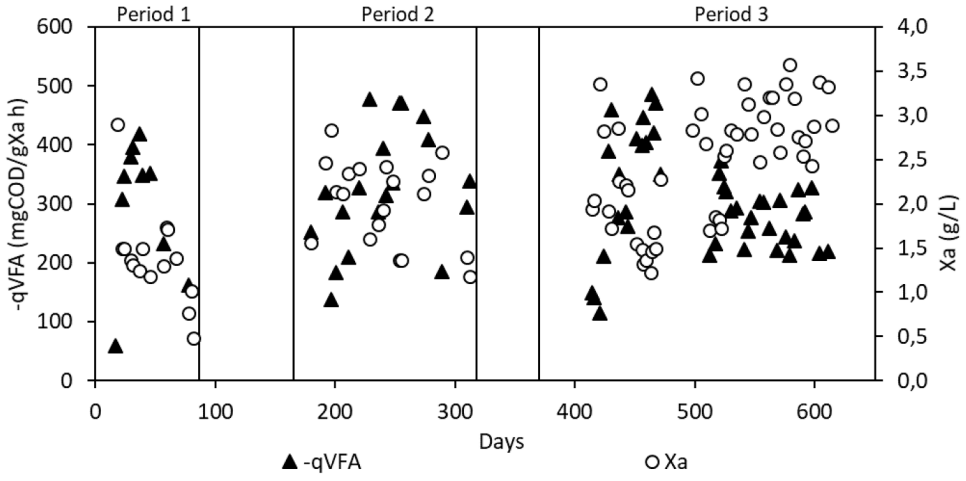

Fig. 3. Substrate uptake rate and Xa concentration among the periods.

Table 8
Substrate uptake rate, PHA and growth yields in the different periods.

Parameter	Unit	Period 1* Average ± st.dev	Period 2 Average ± st.dev	Period 3 Average ± st.dev
$-q_{VFA}^{feast}$	$mgCOD_{VFA}/gXa\ h$	301 ± 38	322 ± 42	289 ± 36
q_{PHA}^{feast}	$mgPHA/gXa\ h$	221 ± 32	231 ± 44	184 ± 21
F/M	$gCOD_{VFA}/gXa\ d$	0.55 ± 0.04	0.57 ± 0.06	0.49 ± 0.04
Y_{obs}	$gXa/gCOD_{VFA}$	0.29 ± 0.02	0.29 ± 0.01	0.31 ± 0.02
$Y_{PHA/VFA}^{feast}$	$gCOD_{PHA}/gCOD_{VFA}$	0.74 ± 0.04	0.72 ± 0.04	0.64 ± 0.16

* Considering only first 38 days of operation

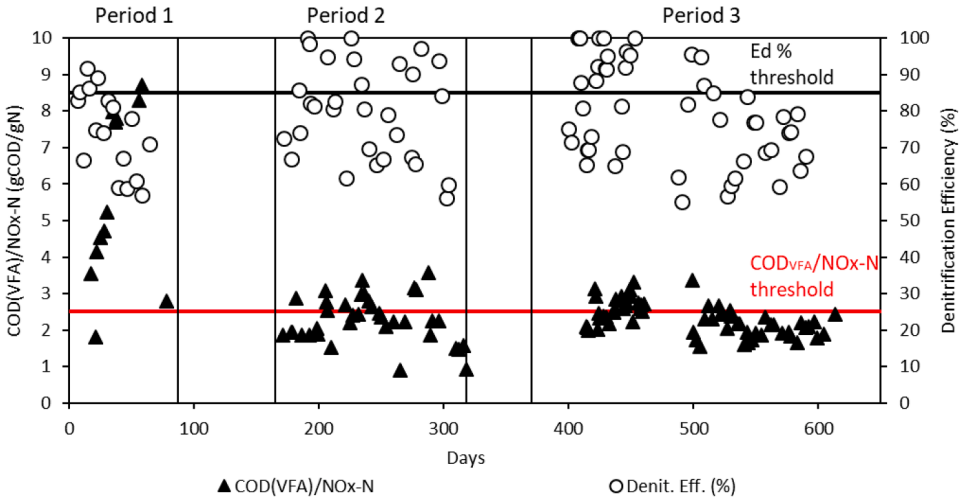

Fig. 4. COD/NO_x-N ratio and denitritation efficiency.

3.4. Cycle profile during PHA biomass selection

Several operating cycles were analyzed throughout the whole monitoring period to assess the process performances. Nitrite, ammonium, VFAs, Xa, PHA and DO profile for a typical cycle of the S-SBR operating during period 2 are reported in Fig. 5.

At the beginning of the (aerobic) feast phase, after the addition of the fermentation liquid, the VFAs concentrations increased up to around 650 mg COD/L. The profile of the DO concentration showed an increase up to 2.5–3.0 mg O_2/L when the aeration started and a suddenly decrease after about 4–5 min; afterward, it stabilized at 0.8–1.0 mg O_2/L for around 45–50 min. This behavior was a consequence of the increased metabolic activity [41], resulting in a VFAs depletion that took place with a rate of around 377 mg $COD_{VFA}/g\ X_a$ h. At the same time, PHA was accumulated within the biomass with a yield of about 0.71 g $COD_{PHA}/g\ COD_{VFA}$, resulting in a PHA concentration of 10% (VSS basis) and 463 mg COD_{PHA}/L, respectively. As soon as almost all the VFAs were consumed within 50 min, the DO concentration started to increase as a response to substrate consumption [14], indicating that the feast phase was about to end. However, the slow DO increase after the consumption of VFAs (from 50 to 70 mins) indicated the presence of some slowly biodegradable COD in the carbon source [11]. After 70 min, anoxic famine conditions were established by means of nitrite feeding and DO depletion, resulting in an

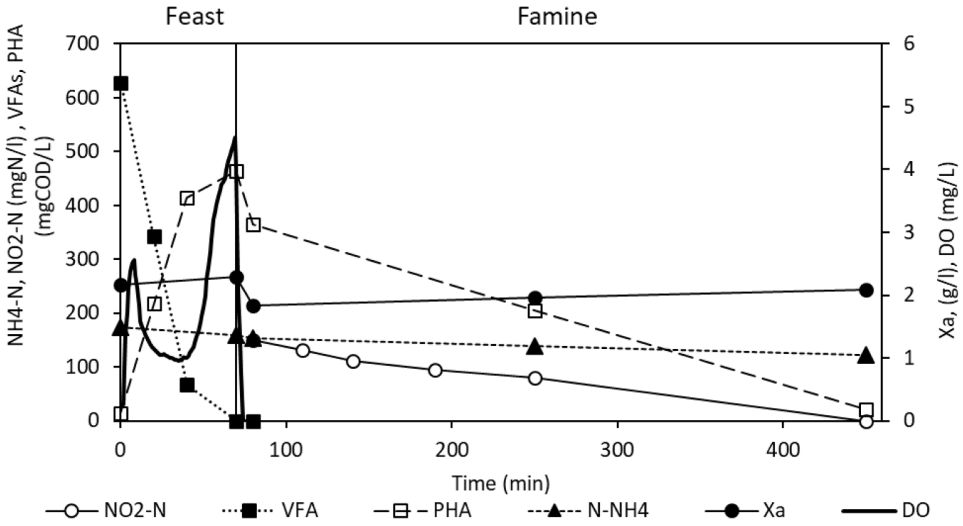

Fig. 5. Cycle profile of S-SBR.

initial concentration of 149 mg NO_2-N/L and an exchange volume ratio of around 0.14 m^3/m^3 reactor. Nitrites were completely depleted after 380 min of famine phase, with a denitritation rate (at 20 °C) of 11.4 mg NO_2-N/g X_a h. The PHA consumption efficiency was > 94%, indicating that the internally stored carbon was effectively used as electron donor for nitrite denitritation, resulting in a PHA content (VSS basis) equal to 0.3% at the end of the cycle. At the same time, the ammonium concentration decreased from 153 to 139 mg NH_4-N/L in relation to the growth of PHA-accumulating bacteria [16].

3.5. PHA accumulation

The first accumulation tests were performed using acetate (COD:N:P = 100:0:0) as a reference carbon source, since it is more favorable for the production of PHAs [42]. With this substrate, the biomass was able to accumulate up to 55% of PHA (VSS basis) with a Y_{PHA} of 0.62 g COD_{PHA}/g COD_{VFA}. Although this value is quite higher compared to other literature studies, it is in agreement with Valentino et al. [12], which reported a Y_{PHA} during accumulation tests carried out with acetate of 0.67 g COD_{PHA}/g COD_{VFA}. The growth yield ranged from 0.11 to 0.16 g Xa/g COD_{VFA}, indicating that a fraction of the substrate was consumed for cell synthesis. This behavior was also reported by Frison et al. [16] and was attributed to the presence of N and P in the liquor withdrawn from the S-SBR that was used as inoculum for the accumulation tests. The produced biopolymer was composed by 100% 3-HB, in agreement with the results reported by Morgan-Sagastume et al. [14]. After acetic acid, PHA production was evaluated without nutrients limitation using real CPSFL (COD:N:P~100:2:0.75) as a carbon source (Fig. 6).

In this case, the PHA concentration (VSS basis) increased up to 42% after almost 4 h and then stabilized. However, after that point, only the mass of both PHA and Xa increased, indicating a shift of carbon utilization towards the synthesis of new biomass cells, as reported by Valentino et al. [43]. The same authors found that under no nutrient limitation, the biomass growth during accumulation tests had benefits on the final PHA production, since it increased the process productivity. Similar results were reported also by Jia et al. [44], where PHA accumulations were performed under nutrient abundance (COD/N = 10). The PHA concentration in the biomass of above 40% wt observed in this study (Table 9), could have a significant impact on further downstream recovery, as it is considered the threshold for the application of economical PHA extraction processes [45]. The Y_{PHA} of the accumulation tests with CPSFL were on average 0.61 and 0.58 g COD_{PHA}/g COD_{VFA} in period 2 and 3, respectively, while the growth yield fluctuated from 0.18 to 0.24 g Xa/g COD_{VFA}. The PHA yields of the current work were higher in comparison with other studies, where PHA production was investigated at pilot scale using fermented feedstocks as carbon source. In those cases, PHA yields varied between 0.25 and 0.51 g COD_{PHA}/g COD_{VFA} (Table 9). On the other hand, the pilot-scale results of this study underline the strength of this process in terms of PHA production and integrated via-nitrite nitrogen removal from reject water.

The use of fermentative VFAs as carbon source affected the characteristics of the recovered biopolymer in terms of HB:HV (w/w) ratio. In this study, the HB content ranged from 59 to 76%, while the HV was found to be between 21 and 41%. Comparing the present results with the work of Frison et al. [16], despite the ratio between even and odd VFAs in the carbon source was quite high (0.34 and 0.49–0.52 mol/mol, respectively), in both cases the HV content was comparable to polymers obtained from carbon sources with lower amount of odd VFAs (Table 6). Carvalho et al. [46] investigated the effects of mixed microbial culture composition on PHAs production using fermented molasses as carbon source. The authors reported that the polymer characteristics (e.g. % HB:HV content) were strongly affected by the operating conditions (e.g. OLR and F/F ratio) which influenced the microbial community of the MMC. Low OLRs in combination with low F/F ratio (i.e. < 0.2 min/min) were found to be favorable for the growth of microorganisms able to synthesize lower fractions of HV. This behavior was attributed by the tendency to operate decarboxylation of propionyl-CoA to acetyl-CoA from these bacteria, as previously reported by Pardelha et al. [47], thus reducing the final HV content. Another parameter that could have affected the polymer composition observed in the present study could have been the pH value in the accumulation phase. Indeed, Kourmenza et al. [48] investigated the effect of pH on PHA composition and the results showed that higher initial pH (e.g. > 7.5) led to lower HV production. This finding could be an explanation to the results observed in the present study, since pH in the accumulation step ranged from 8.0 to 9.5. However, the same authors underlined again the impact that both microbial consortia and operational conditions have on the characteristics of the biopolymer, making somehow difficult the comparison of the results obtained in the present study with other works due to the application of a non-conventional feast/famine process.

3.6. Assessment of the PHAs production potential and economic impact

To better understand the impact of the integration of PHA production in the sidestream treatment line, an overall mass balance was accomplished considering the AD of CPS and WAS as reference scenario. The complete description and calculation behind the results shown in Fig. 7 are reported in the supplementary information. In the reference

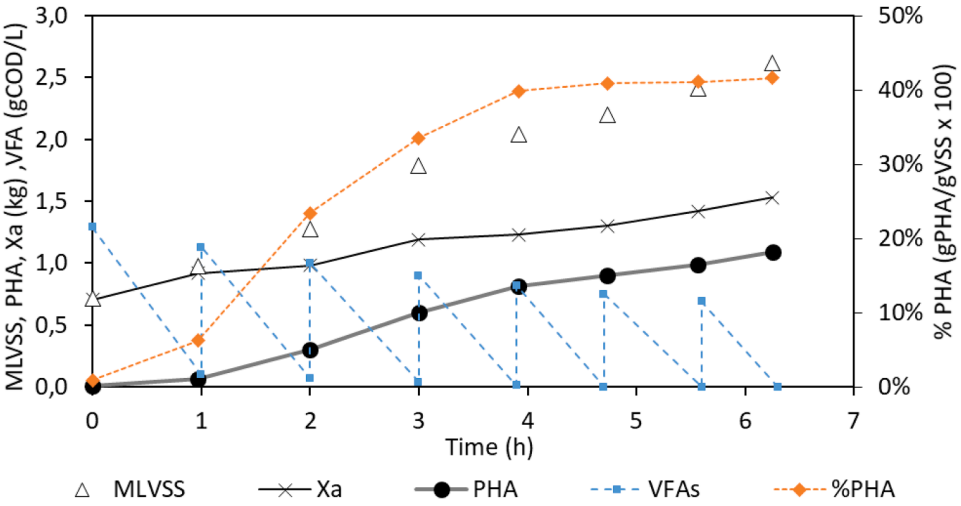

Fig. 6. MLVSS, Xa, and PHA profiles of a typical accumulation test with CPSFL as carbon source.

Table 9
Comparison between different studies using fermented feedstocks for PHA production.

Type of CS	$C_3/(C_2 + C_3)$ (mol/mol)	%PHA (gPHA/gVSS x100)	$Y_{PHA/VFA}$ (gCOD/gCOD)	$Y_{X/VFA}$ (gCOD/gCOD)	PHA produced (kg/batch)	PHAproductivity (mgPHA/L h)	HB:HV(% w/w)	Reference
Acetate (Period 2)	–	46.8 ± 5	0.60 ± 0.06	0.18 ± 0.03	0.88 ± 0.16	269 ± 34	100:0	This study
Acetate	–	40 ± 0.02	0.67 ± 0.05	0.08 ± 0.01	–	200 ± 4	100:0	[12]
CPSFL (Period 2)	0.52 ± 0.06	44.1 ± 6	0.61 ± 0.07	0.28 ± 0.06	0.96 ± 0.10	224 ± 47	59–74:21–41	This study
CPSFL (Period 3)	0.49 ± 0.08	39.6 ± 2	0.58 ± 0.05	0.32 ± 0.05	0.85 ± 0.05	234 ± 37	60–76:24–40	This study
OFMSW + WAS FL	0.15–0.17	43–46	0.44–0.50	0.21–0.22	–	290–360	87–90:10–13	[12]
MWW + WASFL	0.24 ± 0.04	27–38	0.25–0.37	0.22–0.32	–	108–151*	66–72:28–34	[14]
Primary sludge FL	0.24–0.26	38–45	0.31–0.51	–	–	–	55–72:28–45	[45]
Mixed I and II sludge FL	0.34*	19 ± 2	0.40 ± 0.04	0.23 ± 0.06	–	–	56:42**	[16]
Mixed I and II sludge FL	0.29[4]	65.5	–	–	–	–	52:48	[42]

* Calculated considering the data provided by the authors.
** 2% Hydroxyhexanoate.

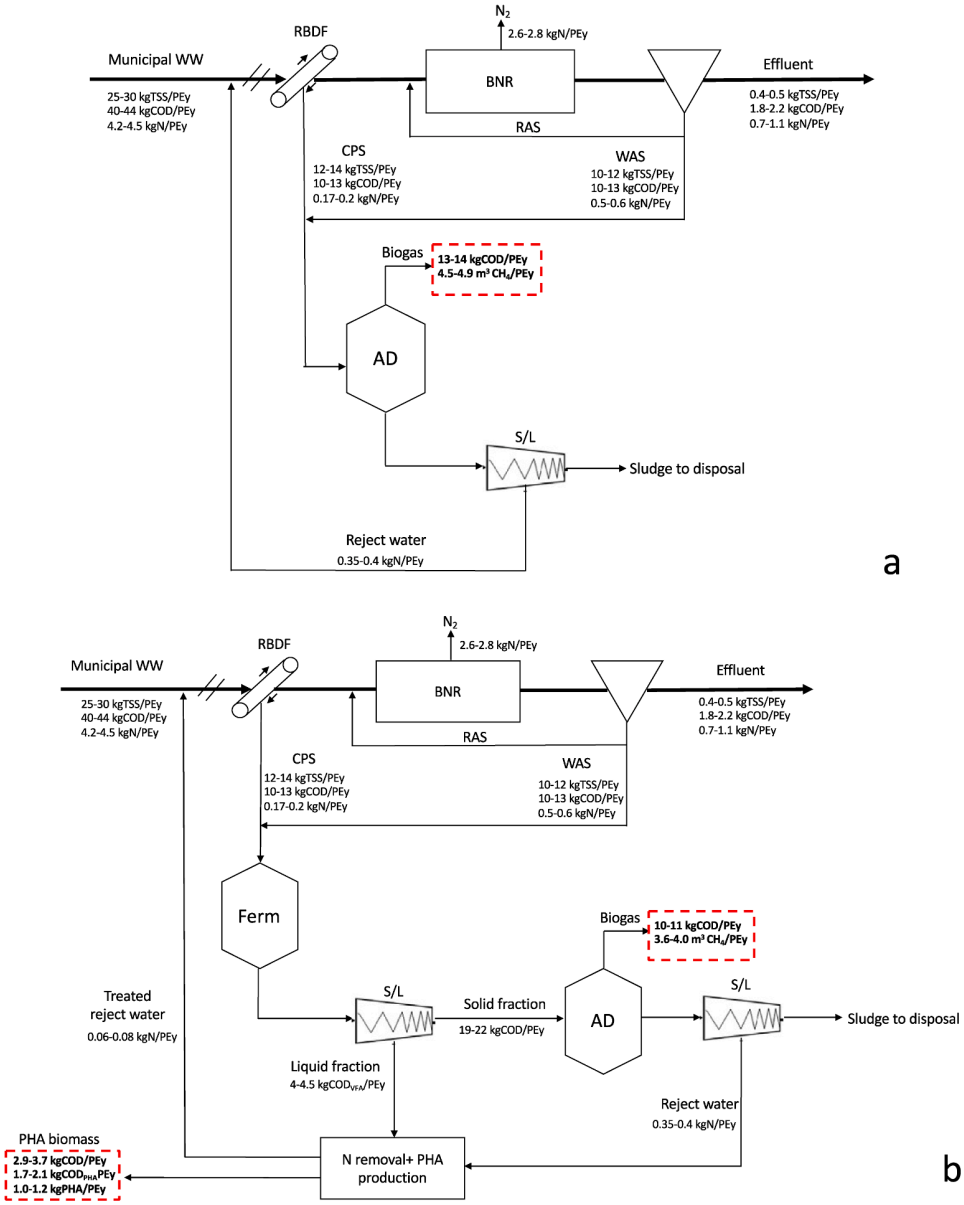

Fig. 7. a) Reference scenario; b) AD and integrated PHA production scenario.

scenario (Fig. 7 a), the CH_4 production recovered from the anaerobic digestion of CPS and secondary sludge was as high as 4.9 m^3CH_4/PE y, corresponding to an overall recovery of 0.32 gCOD per g of COD treated in the municipal WWTPs. The latter is slightly higher than the value reported by Morgan-Sagastume et al. [15], due to the higher biodegradability of the CPS. However, this value is still in the range reported

Table 10
Comparison between recovered COD as biogas and PHA with related income for the different scenarios.

Scenario	AD only		AD & integrated PHA production	
	kgCOD/PE y	€/PE y	kgCOD/PE y	€/PE y
Biogas	13.0–14.0	0.54–0.58	9.9–10.9	0.41–0.45
PHA biomass	–	–	2.9–3.6	–
PHA	–	–	1.7–2.1	2.2–5.9
COD recovered/ Revenue	13.0–14.0	0.54–0.58	12.8–14.6	2.8–6.5

by Tchobanoglous et al. [29], where the maximum amount of recoverable COD was reported to be around 0.35 gCOD per gram of influent COD. In the second scenario (Fig. 7b), the integration of PHAs production with nitrogen removal in the sidestream showed a potential CH_4 recovery up to 4.0 m^3CH_4/PE y. On the other hand, around 2.9–3.7 kg COD/PE y were recovered as PHA biomass, equal to 20–25% of the total recovered COD. The COD fraction as PHA accounted up to 17.5% of the recovered COD, resulting in a potential production of 1.0–1.2 kgPHA/PE y. In agreement with Morgan-Sagastume et al. [15], the conversion yields of the influent COD into by-products was similar in both scenarios regardless if only AD or integrated PHA production was accomplished.

In the reference scenario, the only revenues come from the biogas production (Table 10). Considering a CH_4 market price of 0.12 €/m^3 (0.04 €/kg COD_{CH4} [49]), the recovered COD would be valorized as high as of 0.58 €/PE per year. On the other hand, although CH_4 production is slightly lower when AD is integrated with PHA production, the impact on the total profit is almost negligible. Indeed, since the market price of PHA ranges from 2 to 5 €/kg PHA [7,8,50], the COD conversion into PHAs could be valorized from 30 to 70 times more in respect to CH_4. When PHAs production is integrated with AD, the global revenue would range from 2.8 to 6.5 €/PE y, up to 11 times higher than reference scenario. Considering that the COD fraction of recovered PHAs represents only 11–18% of the total recovered COD, it appears immediately clear that the implementation of a sidestream technology able to integrate nitrogen removal and PHA production can significantly increase the WWTPs revenue.

4. Conclusions

The upgrade of existing wastewater treatment plants aiming at the resource recovery starts from the on-site production of VFAs through acidogenic fermentation, which are the suitable carbon source for both energy-efficient nutrients removal and PHAs production. Specifically, the present study evaluated both the feasibility and the potential of PHAs production and nitrogen removal from the sidestream of WWTPs at pilot scale by the use of CPS as a novel carbon source. The results showed that around 80% of the influent ammonia was efficiently removed by the system when both the N-SBR and S-SBR operated under vNLR of 1.64–1.72 kgN/m^3d and 0.60–0.63 kgN/m^3d, respectively. Meanwhile, the PHA-accumulating biomass selection was successfully accomplished by means of aerobic-feast and anoxic-famine regime, as shown by the good PHA yields observed in the accumulation batches (0.58–0.61 $gCOD_{PHA}/gCOD_{VFA}$). The overall mass balance assessment pointed that up to 0.32 gCOD per gram of COD treated can be recovered as bio-based product (i.e. CH_4, PHA, or both), regardless of the reference scenario. If only AD is accomplished up to 4.9 m^3CH_4/PE per year can be produced, resulting in a final revenue of 0.58 €/PE y. On the other hand, the integration of AD with PHAs recovery in the sludge line can boost the revenues up to 11 times more with a final income up to 6.5 €/PE y. The PHA production potential assessed in this study demonstrated that up to 1.2 kgPHA/PE y can be produced when treating the sole municipal wastewater. The application of an aerobic-feast and anoxic-famine regime can decrease the energy requirements for PHAs production due to its integration with the via-nitrite nitrogen removal from the anaerobic reject water, boosting the conversion of WWTPs towards WRRFs.

Declaration of Competing Interest

The authors declare that they have no known competing financial interests or personal relationships that could have appeared to influence the work reported in this paper.

Acknowledgments

This study was supported by the “SMART-Plant” Innovation Action (www.smart-plant.eu) which has received funding from the European Union's Horizon 2020 research and innovation programme under grant agreement No 690323. The public utility Alto Trevigiano Servizi Srl is kindly acknowledged for hosting of the experimental facilities within the Carbonera WWTP.

Appendix A. Supplementary data

Supplementary data to this article can be found online at https://doi.org/10.1016/j.cej.2020.124625.

References

[1] C. Puchongkawarin, C. Gomez-Mont, D.C. Stuckey, B. Chachuat, Optimization-based methodology for the development of wastewater facilities for energy and nutrient recovery, Chemosphere 140 (2015) 150–158, https://doi.org/10.1016/j.chemosphere.2014.08.061.
[2] W. Dai, X. Xu, B. Liu, F. Yang, Toward energy-neutral wastewater treatment: A membrane combined process of anaerobic digestion and nitritation-anammox for biogas recovery and nitrogen removal, Chem. Eng. J. 279 (2015) 725–734, https://doi.org/10.1016/j.cej.2015.05.036.
[3] D. Puyol, D.J. Batstone, T. Hülsen, S. Astals, M. Peces, J.O. Krömer, Resource Recovery from Wastewater by Biological Technologies: Opportunities, Challenges, and Prospects, Front. Microbiol. 7 (2017) 2106, https://doi.org/10.3389/fmicb.2016.02106.
[4] W. Tu, D. Zhang, H. Wang, Z. Lin, Polyhydroxyalkanoates (PHA) production from fermented thermal-hydrolyzed sludge by PHA-storing denitrifiers integrating PHA accumulation with nitrate removal, Bioresour. Technol. 292 (2019) 121895, , https://doi.org/10.1016/j.biortech.2019.121895.
[5] E.R. Coats, F.J. Loge, M.P. Wolcott, K. Englund, A.G. McDonald, Synthesis of Polyhydroxyalkanoates in Municipal Wastewater Treatment, Water Environ. Res. 79 (2007) 2396–2403, https://doi.org/10.2175/106143007X183907.
[6] D. Dionisi, M. Majone, V. Papa, M. Beccari, Biodegradable Polymers From Organic Acids by Using Activated Sludge Enriched by Aerobic Periodic Feeding, Biotechnol. Bioeng. 85 (2004) 569–579, https://doi.org/10.1002/bit.10910.
[7] F. Valentino, F. Morgan-Sagastume, S. Campanari, M. Villano, A. Werker, M. Majone, Carbon recovery from wastewater through bioconversion into biodegradable polymers, New Biotechnol. 37 (2017) 9–23, https://doi.org/10.1016/j.nbt.2016.05.007.
[8] N.R. de Hart, E.D. Bluemink, A.J. Geilvoet, J.F. Kramer, Bioplastic from sludge. Exploring PHA production from sewage sludge (Raw materials factory), STOWA report, Amersfoort, 2014.
[9] European Bioplastics Association. https://www.european-bioplastics.org/market/, 2020 (assessed 26 February 2020).
[10] M.H. Madkour, D. Heinrich, M.A. Alghamdi, I.I. Shabbaj, A. Steinbüchel, PHA recovery from biomass, Biomacromolecules 14 (2013) 2963–2972, https://doi.org/10.1021/bm4010244.
[11] S. Anterrieu, L. Quadri, B. Geurkink, I. Dinkla, S. Bengtsson, M. Arcos-Hernandez, T. Alexandersson, F. Morgan-Sagastume, A. Karlsson, M. Hjort, L. Karabegovic, P. Magnusson, P. Johansson, M. Christensson, A. Werker, Integration of biopolymer production with process water treatment at a sugar factory, New Biotechnol. 31 (2014) 308–323, https://doi.org/10.1016/j.nbt.2013.11.008.
[12] F. Valentino, G. Moretto, L. Lorini, D. Bolzonella, P. Pavan, M. Majone, Pilot-scale polyhydroxyalkanoate production from combined treatment of organic fraction of municipal solid waste and sewage sludge, Ind. Eng. Chem. Res. 58 (2019) 12149–12158, https://doi.org/10.1021/acs.iecr.9b01831.
[13] S. Bengtsson, A. Karlsson, T. Alexandersson, L. Quadri, M. Hjort, P. Johansson, F. Morgan-Sagastume, S. Anterrieu, M. Arcos-Hernandez, L. Karabegovic, P. Magnusson, A. Werker, A process for polyhydroxyalkanoate (PHA) production from municipal wastewater treatment with biological carbon and nitrogen removal demonstrated at pilot-scale, New Biotechnol. 35 (2017) 42–53, https://doi.org/10.1016/j.nbt.2016.11.005.
[14] F. Morgan-Sagastume, M. Hjort, D. Cirne, F. Gérardin, S. Lacroix, G. Gaval,

L. Karabegovic, T. Alexandersson, P. Johansson, A. Karlsson, S. Bengtsson, M.V. Arcos-Hernández, P. Magnusson, A. Werker, Integrated production of polyhydroxyalkanoates (PHAs) with municipal wastewater and sludge treatment at pilot scale, Bioresour. Technol. 181 (2015) 78–89, https://doi.org/10.1016/j.biortech.2015.01.046.

[15] F. Morgan-Sagastume, S. Heimersson, G. Laera, A. Werker, M. Svanström, Techno-environmental assessment of integrating polyhydroxyalkanoate (PHA) production with services of municipal wastewater treatment, J. Cleaner Prod. 137 (2016) 1368–1381, https://doi.org/10.1016/j.jclepro.2016.08.008.

[16] N. Frison, E. Katsou, S. Malamis, A. Oehmen, F. Fatone, Development of a novel process integrating the treatment of sludge reject water and the production of Polyhydroxyalkanoates (PHAs), Environ. Sci. Technol. 49 (2015) 10877–10885, https://doi.org/10.1021/acs.est.5b01776.

[17] W.S. Lee, A.S.M. Chua, H.K. Yeoh, G.C. Ngoh, A review of the production and application of waste-derived volatile fatty acids, Chem. Eng. J. 235 (2014) 83–99, https://doi.org/10.1016/j.cej.2013.09.002.

[18] D. Crutchik, N. Frison, A.L. Eusebi, F. Fatone, Biorefinery of cellulosic primary sludge towards targeted Short Chain Fatty Acids, phosphorus and methane recovery, Water Res. 136 (2018) 112–119, https://doi.org/10.1016/j.watres.2018.02.047.

[19] C. Da Ros, V. Conca, A.L. Eusebi, N. Frison, F. Fatone, Sieving of municipal wastewater and recovery of bio-based volatile fatty acids at pilot scale, Water Res. 174 (2020) 115633, , https://doi.org/10.1016/j.watres.2020.115633.

[20] S. Longo, N. Frison, D. Renzi, F. Fatone, A. Hospido, Is SCENA a good approach for side-stream integrated treatment from an environmental and economic point of view? Water Res. 125 (2017) 478–489, https://doi.org/10.1016/j.watres.2017.09.006.

[21] A.C. Anthonisen, R.C. Loehr, T.B.S. Prakasam, E.G. Srinath, Inhibition of Nitrification by Ammonia and Nitrous Acid, J. Water Pollut. Control Fed. 48 (1976) 835–852 https://www.jstor.org/stable/25038971.

[22] E.R. Coats, B.S. Watson, C.K. Brinkman, Polyhydroxyalkanoate synthesis by mixed microbial consortia cultured on fermented dairy manure: Effect of aeration on process rates/yields and the associated microbial ecology, Water Res. 106 (2016) 26–40, https://doi.org/10.1016/j.watres.2016.09.039.

[23] D. Dionisi, M. Majone, G. Vallini, S. Di Gregorio, M. Beccari, Effect of the length of the cycle on biodegradable polymer production and microbial community selection in a sequencing batch reactor, Biotechnol. Prog. 23 (2007) 1064–1073, https://doi.org/10.1021/bp060370c.

[24] F. Morgan-Sagastume, F. Valentino, M. Hjort, D. Cirne, L. Karabegovic, F. Gerardin, P. Johansson, A. Karlsson, P. Magnusson, T. Alexandersson, S. Bengtsson, M. Majone, A. Werker, Polyhydroxyalkanoate (PHA) production from sludge and municipal wastewater treatment, Water Sci. Technol. 69 (2014) 177–184, https://doi.org/10.2166/wst.2013.643.

[25] APHA, AWWA, WEF, Standard Methods for the Examinations of Water and Wastewater, 20th Edition, American Public Health Association, Washington, 1998.

[26] APAT, IRSA-CNR, Analytical Methods for Water, APAT Guidelines and Manuals, Reports 29/2003, Rome, 2003.

[27] G. Braunegg, B. Sonnleitner, R.M.A. Lafferty, Rapid gas chromatographic method for the determination of poly-b-hydroxybutyric acid in microbial biomass, Eur. J. Appl. Microbiol. 6 (1978) 29–37, https://doi.org/10.1007/BF00500854.

[28] P. Battistoni, F. Fatone, E. Cola, P. Pavan, Alternate cycles process for municipal WWTPs upgrading: Ready for widespread application? Ind. Eng. Chem. Res. 47 (2008) 4387–4393, https://doi.org/10.1021/ie070109g.

[29] G. Tchobanoglous, H.D. Stensel, R. Tsuchihashi, F.L. Burton, M. Abu.Orf, G. Bowden, W. Pfrang, Wastewater Engineering Treatment and Reuse, 5th Edition, Metcalf & Eddy Inc., McGraw-Hill Education, New York, 2014.

[30] Y. Shao, S. Yang, A. Mohammed, Y. Liu, Impacts of ammonium loading on nitritation stability and microbial community dynamics in the integrated fixed-film activated sludge sequencing batch reactor (IFAS-SBR), Int. Biodeterior. Biodegrad. 133 (2018) 63–69, https://doi.org/10.1016/j.ibiod.2018.06.002.

[31] H. Salehizadeh, M.C.M. Van Loosdrecht, Production of polyhydroxyalkanoates by mixed culture: recent trends and biotechnological importance, Biotechnol. Adv. 22 (2004) 261–279, https://doi.org/10.1016/j.biotechadv.2003.09.003.

[32] J. Wu, C. He, M.C.M. Van Loosdrecht, J. Pérez, Selection of ammonium oxidizing bacteria (AOB) over nitrite oxidizing bacteria (NOB) based on conversion rates, Chem. Eng. J. 304 (2016) 953–961, https://doi.org/10.1016/j.cej.2016.07.019.

[33] I. Jubany, J. Lafuente, J.A. Baeza, J. Carrera, Total and stable washout of nitrite oxidizing bacteria from a nitrifying continuous activated sludge system using automatic control based on Oxygen Uptake Rate measurements, Water Res. 43 (2009) 2761–2772, https://doi.org/10.1016/j.watres.2009.03.022.

[34] X. Wang, A. Oehmen, E.B. Freitas, G. Carvalho, M.A.M. Reis, The link of feast-phase dissolved oxygen (DO) with substrate competition and microbial selection in PHA production, Water Res. 112 (2017) 269–278, https://doi.org/10.1016/j.watres.2017.01.064.

[35] E. Korkakaki, M. Mulders, A. Veeken, R. Rozendal, M.C.M. Van Loosdrecht, R. Kleerebezem, PHA production from the organic fraction of municipal solid waste (OFMSW): overcoming the inhibitory matrix, Water Res. 96 (2016) 74–83, https://doi.org/10.1016/j.watres.2016.03.033.

[36] F. Valentino, M. Gottardo, F. Micolucci, P. Pavan, D. Bolzonella, S. Rossetti, M. Majone, Organic fraction of municipal solid waste recovery by conversion into added-value polyhydroxyalkanoates and biogas, ACS Sustain. Chem. Eng. 6 (2018) 16375–16385, https://doi.org/10.1021/acssuschemeng.8b03454.

[37] M.G.E. Albuquerque, C.A.V. Torres, M.A.M. Reis, Polyhydroxyalkanoate (PHA) production by a mixed microbial culture using sugar molasses: effect of the influent substrate concentration on culture selection, Water Res. 44 (2010) 3419–3433, https://doi.org/10.1016/j.watres.2010.03.021.

[38] E. Korkakaki, M.C.M. Van Loosdrecht, R. Kleerebezem, Impact of phosphate limitation on PHA production in a feast-famine process, Water Res. 126 (2017) 472–480, https://doi.org/10.1016/j.watres.2017.09.031.

[39] M. Henze, W. Gujer, T. Mino, M.C.M. Van Loosdrecht, Activated Sludge Models ASM1, ASM2, ASM2d, and ASM3, IWA Scientific and Technical Report n.9, IWA Publishing, London, 2000.

[40] N. Frison, S. Lampis, D. Bolzonella, P. Pavan, F. Fatone, Two-stage start-up to achieve the stable via-nitrite pathway in a demonstration SBR for anaerobic codigestate treatment, Ind. Eng. Chem. Res. 51 (2012) 15423–15430, https://doi.org/10.1021/ie3009742.

[41] S. Campanari, F. Augelletti, S. Rossetti, F. Sciubba, M. Villano, M. Majone, Enhancing a multi-stage process for olive oil mill wastewater valorization towards polyhydroxyalkanoates and biogas production, Chem. Eng. J. 317 (2017) 280–289, https://doi.org/10.1016/j.cej.2017.02.094.

[42] Y. Chen, M. Li, F. Meng, W. Yang, L. Chen, M. Huo, Optimal poly (3-hydroxybutyrate/3-hydroxyvalerate) biosynthesis by fermentation liquid from primary and waste activated sludge, Environ. Technol. 35 (2014) 1791–1801, https://doi.org/10.1080/09593330.2014.882993.

[43] F. Valentino, L. Karabegovic, M. Majone, F. Morgan-Sagastume, A. Werker, Polyhydroxyalkanoate (PHA) storage within a mixed-culture biomass with simultaneous growth as a function of accumulation substrate nitrogen and phosphorus levels, Water Res. 77 (2015) 49–63, https://doi.org/10.1016/j.watres.2015.03.016.

[44] Q. Jia, H. Wang, X. Wang, Dynamic synthesis of polyhydroxyalkanoates by bacterial consortium from simulated excess sludge fermentation liquid, Bioresour. Technol. 140 (2013) 328–336, https://doi.org/10.1016/j.biortech.2013.04.105.

[45] A. Werker, S. Bengtsson, L. Korving, M. Hjort, S. Anterrieu, T. Alexandersson, P. Johansson, A. Karlsson, L. Karabegovic, P. Magnusson, F. Morgan, L. Sagastume, M. Sijstermans, C. Tietema, E. Visser, Y. van der Wypkema, A. Deeke Kooij, C. Uijterlinde, Consistent production of high quality PHA using activated sludge harvested from full scale municipal wastewater treatment – PHARIO, Water Sci. Technol. 78 (2018) 2256–2269, https://doi.org/10.2166/wst.2018.502.

[46] G. Carvalho, A. Oehmen, M.G.E. Albuquerque, M.A.M. Reis, The relationship between mixed microbial culture composition and PHA production performance from fermented molasses, New Biotechnol. 31 (2014) 257–263, https://doi.org/10.1016/j.nbt.2013.08.010.

[47] F. Pardelha, M.G.E. Albuquerque, M.A.M. Reis, J.M.L. Dias, R. Oliveira, Flux balance analysis of mixed microbial cultures: Application to the production of polyhydroxyalkanoates from complex mixtures of volatile fatty acids, J. Biotechnol. 162 (2012) 336–345, https://doi.org/10.1016/j.jbiotec.2012.08.017.

[48] C. Kourmentza, M. Kornaros, Biotransformation of volatile fatty acids to polyhydroxyalkanoates by employing mixed microbial consortia: The effect of pH and carbon source, Bioresour. Technol. 222 (2016) 388–398, https://doi.org/10.1016/j.biortech.2016.10.014.

[49] U.S. Energy Information Administration, United States Natural Gas Industrial Price. https://www.eia.gov/dnav/ng/hist/n3035us3m.htm, 2019 (accessed 22 November 2019).

[50] R. Kleerebezem, B. Joose, R. Rozendal, M.C.M. Van Loosdrecht, Anaerobic digestion without biogas? Rev. Environ. Sci. Biotechnol. 14 (2015) 787–801, https://doi.org/10.1007/s11157-015-9374-6.